observers, without retinal motion. In the first situation, five subjects (two authors and three naive subjects) wearing the helmet of an eye-tracking system (Senso-Motoric Eyelink) focused their gaze on a vertical bar made up of light-emitting diodes (LEDs). The bar was mounted on the helmet 36 cm in front of the eyes. In complete darkness, subjects were instructed to rotate their heads horizontally back and forth (at 20–30 degrees, with a rhythm of about 0.3–0.4 Hz). The lower two-thirds of the bar (26 mm × 1.5 mm) was continuously lit, while the upper one-third of the bar was flashed for 6 ms halfway through the head movements.

The recordings showed that, while gaze (the position of the eye in space) moved approximately 25 degrees per cycle (Fig. 1), the total eye displacements relative to the head were less than 1 degree per cycle. Furthermore, no eye displacement in the head occurred at the time of the flashes, so the motion of the stimulus on the retina was minimal compared with the motion of the stimulus in space.

When the subjects were asked to judge the position of the array with respect to the position of the flashed LEDs, however, they invariably reported that the continuously lit LEDs were ahead of the flashed ones. Even though all subjects, including the naive ones, had seen the LED array before the experiment and knew that all the LEDs were fixed on a single rigid bar, they still perceived a misalignment of several degrees of visual angle between the continuously lit and the flashing segments, as in earlier studies in which there was retinal motion[1,2]. When the subjects were continuously rotated in a chair at 20 revolutions per minute, the visual stimulus was the same. The continuously lit moving stimulus was seen as leading, most clearly at the start of rotation, and as lagging during the final deceleration.

The brain has no direct access to the timing of external events because input delays are variable and therefore unreliable[3]. When moving stimuli are involved, uncertainty about the time of an event (for example, of a flash) can translate into uncertainty about position. The time–position ambiguity resulting from processing delays may affect the perception of stimulus motion, regardless of how the brain has access to this information. Whether the cue derives from retinal, oculomotor, vestibular or proprioceptive signals, the perceived position of a moving object may be extrapolated in the same way.

John Schlag, Rick H. Cai, Andrews Dorfman, Ali Mohempour, Madeleine Schlag-Rey

Department of Neurobiology, School of Medicine, UCLA, Los Angeles, California 90095, USA

e-mail: jschlag@ucla.edu

1. Nijhawan, R. *Nature* **370,** 256–257 (1994).
2. Nijhawan, R. *Nature* **386,** 66–69 (1997).
3. Purushothaman, G., Patel, S. S., Bedell, H. E. & Ogmen, H. *Nature* **396,** 424 (1998).
4. Whitney, D. & Murakami, I. *Nature Neurosci.* **1,** 656–657 (1998).
5. Gegenfurtner, K. *Nature* **398,** 291–292 (1999).
6. Berry, M. J., Brivanlou, I. H., Jordan, T. A. & Meister, M. *Nature* **398,** 334–338 (1999).

Cognition

Numerical memory span in a chimpanzee

A female chimpanzee called Ai has learned to use Arabic numerals to represent numbers[1]. She can count from zero to nine items, which she demonstrates by touching the appropriate number on a touch-sensitive monitor[2,3], and she can order the numbers from zero to nine in sequence[4–6]. Here we investigate Ai's memory span by testing her skill in these numerical tasks, and find that she can remember the correct sequence of any five numbers selected from the range zero to nine.

Humans can easily memorize strings of codes such as phone numbers and postcodes if they consist of up to seven items, but above this number they find it much harder. This 'magic number 7' effect, as it is known in human information processing[7], represents a limit for the number of items that can be handled simultaneously by the brain.

To determine the equivalent 'magic number' in a chimpanzee, we presented our subject with a set of numbers on a screen, say 1, 3, 4, 6 and 9. She had already displayed close to perfect accuracy when required to choose numerals in ascending order, but for this experiment all the remaining numbers were masked by white squares once she had selected the first number. This meant that, in order to be correct in a trial, she had to memorize all the numbers, as well as their respective positions, before making the first response. Chance levels with three, four and five items were 50, 13 and 6%, respectively.

Ai scored more than 90% with four items and about 65% with five items, significantly above chance in each case. In normal background trials, response latency was longest for the first numeral and much shorter for all the others, indicating that Ai inspected the numbers and their locations and planned her actions before making her first choice. In masking trials, response latency increased only for the choice directly after the onset of masking, but this latency was similar to those recorded in background trials, indicating that successful performance did not depend on spending more time memorizing the numbers.

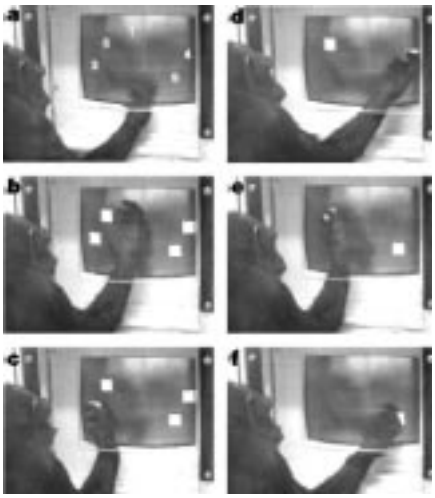

Figure 1 The chimpanzee Ai performing the five-number ordering task in the 'masking' trial. Five numbers (1, 3, 4, 6 and 9) are presented on the touch-sensitive monitor. **a, b,** Ai correctly chooses the number 1 as the lowest of the series (**a**), at which point the remaining numbers are automatically masked (**b**). **c–f,** She continues to identity the numbers one by one in ascending order (**c–e**), ending with the 9 (**f**). See Supplementary Information and http://www.pri.kyoto-u.ac.jp for more details.

In one testing session, after Ai had chosen the correct number and all the remaining items were masked by white squares, a fight broke out among a group of chimpanzees outside the room, accompanied by loud screaming. Ai abandoned her task and paid attention to the fight for about 20 seconds, after which she returned to the screen and completed the trial without error.

Ai's performance shows that chimpanzees can remember the sequence of at least five numbers, the same as (or even more than) preschool children. Our study and others[8–10] demonstrate the rudimentary form of numerical competence in non-human primates.

Nobuyuki Kawai, Tetsuro Matsuzawa

Primate Research Institute, Kyoto University,

Table 1 Performance in masking trials

			Number (% correct)						Response time (ms)				
Type of trial	*Numbers*	*Trials*	*1st*	*2nd*	*3rd*	*4th*	*5th*	*Total*	*1st*	*2nd*	*3rd*	*4th*	*5th*
Normal	2	405	98	100	—	—	—	98	676	420	—	—	—
Normal	3	433	97	97	100	—	—	94	710	424	420	—	—
Normal	4	451	93	96	98	100	—	87	754	439	407	412	—
Normal	5	421	90	93	94	99	100	78	799	448	415	430	408
Masking	3	200	98	91	100	—	—	89	768	533	465	—	—
Masking	4	20	100	100	95	100	—	95	717	390	432	437	—
Masking	5	20	95	95	89	81	100	65	721	446	426	466	411

1st, 2nd, 3rd, 4th and 5th refer to the numbers in a sequence in ascending order.

Inuyama, Aichi 484-8506, Japan
e-mail: matsuzaw@pri.kyoto-u.ac.jp

1. Matsuzawa, T. *Nature* **315,** 57–59 (1985).
2. Matsuzawa, T., Itakura, S. & Tomonaga, M. in *Primatology Today* (eds Ehara, A., Kumura, T., Takenaka, O. & Iwamoto, M.) 317–320 (Elsevier, Amsterdam, 1991).
3. Murofushi, K. *Jpn. Psychol. Res.* **39,** 140–153 (1997).
4. Tomonaga, M., Matsuzawa, T. & Itakura, S. *Primate Res.* **9,** 67–77 (1993).
5. Biro, D. & Matsuzawa, T. *J. Comp. Psychol.* **113,** 178–185 (1999).
6. Tomonaga, M. & Matsuzawa, T. *Anim. Cogn.* (in the press).
7. Miller, G. A. *Psychol. Rev.* **63,** 81–97 (1956).
8. Rumbaugh, D., Savage-Rumbaugh, E. S. & Hegel, M. *J. Exp. Psychol. Anim. Behav. Process.* **13,** 107–115 (1987).
9. Brannon, E. & Terrace, H. *Science* **282,** 746–749 (1998).
10. Boysen, S., Mukobi, K. & Berntson, G. *Anim. Learn. Behav.* **27,** 229–235 (1999).

Supplementary information is available on *Nature*'s World-Wide Web site (http://www.nature.com) or as paper copy from the London editorial office of *Nature*.

Medical physics

Explaining the T-wave shape in the ECG

The heartbeat is recorded on an electrocardiogram (ECG) as a characteristic trace determined by changes in the electrical activity of the heart muscle. The T wave is a component of this waveform that is associated with the repolarization phase of the action potentials[1]. It is asymmetrical in healthy subjects, but tends to become symmetrical with heart disease[2]. The reason for the T-wave shape is not clear[3]. Here we show that T waves become more symmetrical as a result of an increase in the dispersion of the regional repolarization of cardiac muscle.

The exact sequence of depolarization and repolarization of the action potential (the potential difference that arises between the intracellular and extracellular fluid) in three-dimensional heart muscle is complex, but to model the electrocardiogram on the body surface, only the heart surface potentials need to be known[4], assuming that the myocardium has uniform and isotropic conductivity. Although the repolarization on any individual cell is timed to the initiation of its action potential, repolarization occurs smoothly and systematically across the epicardial surface[5,6]. Repolarization of the surface of the left ventricle occurs first epicardially in the postero-basal region, then at the septal wall and apex[6], and finally at the endocardial surface[7].

We used this spatial sequence on a simple model of the left ventricle which allowed the body-surface 12-lead T waves of the ECG to be calculated with the standard repolarization phases of an action potential[8] and standard modelling equations[4]. The body was represented by an elliptical cylinder[9]and the heart by a truncated ellipsoid (axis diameters, 7.0 and 6.6 cm; height from base, 7.4 cm; displaced 4 cm left and 6 cm forward of the body axis, and rotated 25 degrees forward and 40 degrees to the left).

We evaluated this model twice: by using a fixed, normal shape for the action potential, and then by using three regions, each with a different shape for the action potential, with a 10% increase in model parameters[8] at the endocardium and with a 10% decrease at the apex. These changes to the parameters generated abnormally shaped action potentials. To make sure that the results did not depend on the specific model values, we calculated the form of T waves for the initial heart position and for separate shifts of the axes of ± 2 cm and rotations of ± 10 degrees, to calculate error bars.

To represent differences in the regional dispersion of repolarization times, we varied the time delay between the first and last action potentials, and thus between the earliest and latest region to repolarize, from 10 to 150 ms in steps of 10 ms, which ranges from normal to abnormal dispersion, and linearly interpolated the time delays for intermediate regions. We calculated a symmetry ratio from the body-surface T waves as the ratio of the areas under the two sections of the T curves (beginning-to-peak compared with peak-to-end).

Our results show that low dispersion is represented by asymmetrical T waves, and high dispersion by increasingly tall and symmetrical, clinically hyperacute T waves that tend to a symmetry ratio of unity (Fig. 1). This agrees with the accepted symmetry ratio for normal T waves of 1.5 (ref. 10) and with the expected relation between tall, symmetrical T waves and abnormal repolarization. Abnormal shapes in the action potential result in differences in the T-wave symmetry ratio, but still tend to produce symmetrical T waves for high dispersion.

This finding can be explained by considering a simplified situation, based on the assumption that the heart contains only two regions, which give rise to action potentials that have identical shapes but are displaced in time. The resulting potential gradients, and ultimately the shape of the T wave, can be approximated to the difference between the two action potentials at each instant. When dispersion, or time displacement, is small, this difference will result in an asymmetrical waveform (as a consequence of the shape of the action-potential repolarization phase), and when it is large (with the second action potential beginning to repolarize after the first has mostly repolarized), a symmetrical waveform will tend to be produced.

Such a simple model can be expressed mathematically and computed easily but is not convincing without the calculations used here, with more realistic heart and torso geometries and gradual differences in the initiation of action-potential repolarization across the myocardium. Confidence in the model is increased by the resulting T-wave shapes in the 12 ECG leads.

Analysis of T-wave symmetry offers a new clinical indication of dispersion, which would be valuable for patients with high dispersion, who are more likely to die suddenly[11]; the current methods used to measure dispersion are unsatisfactory and are prone to errors[12]. Our results indicate that there is a link between T-wave symmetry and the abnormal regional dispersion of repolarization.

Diego di Bernardo, Alan Murray
Regional Medical Physics Department, Newcastle University, Freeman Hospital, Newcastle upon Tyne NE7 7DN, UK

1. Noble, D. & Cohen, I. R. A. *Cardiovasc. Res.* **12,** 13–27 (1978).
2. Conover, M. B. *Understanding Electrocardiography: Arrhythmias and the 12-lead ECG* (Mosby Year Book, St Louis, Missouri, 1992).
3. Yan, G.-X. & Antzelevitch, C. *Circulation* **98,** 1928–1936 (1998).
4. Simms, H. D. & Geselowitz, D. B. *J. Cardiovasc. Electrophysiol.* **6,** 522–531 (1995).
5. Franz, M. R., Bargheer, K., Rafflenbeul, W., Haverich, A. & Lichten, P. R. *Circulation* **75,** 379–386 (1987).
6. Cowan, J. C. *et al. Br. Heart J.* **60,** 424–433 (1988).
7. Higuchi, T. & Nakaya, Y. *Am. Heart J.* **108,** 290–295 (1984).
8. Wohlfart, B. *Eur. Heart J.* **8,** 409–416 (1987).
9. Gelernter, H. L. & Swihart, J. C. *Biophys. J.* **4,** 285–301 (1964).
10. Merri, M., Benhorin, J., Alberti, M., Locati, E. & Moss, A. J. *Circulation* **80,** 1301–1308 (1989).
11. Barr, C. S. *et al. Lancet* **343,** 327–329 (1994).
12. Murray, A. *et al. Br. Heart J.* **71,** 386–390 (1994).

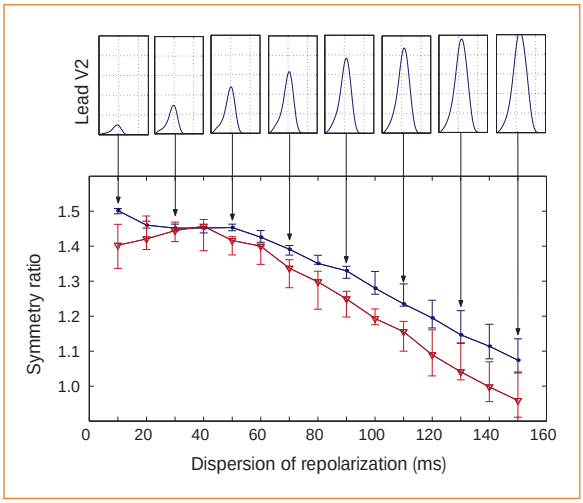

Figure 1 T-wave symmetry ratios for a range of dispersions of repolarization for the two implementations of the model (blue circles, single action potential; red triangles, three regions with different APs) for the mean of precordial leads V2 to V6. V1 was omitted as it was sometimes biphasic. Lines are drawn through the symmetry ratios for the initial heart position; error bars give the maximum range calculated for the different heart positions. The mean difference between limb and precordial leads for the symmetry ratio was 0.026 for the model of the single action potential, and 0.005 for three action potentials. The graphs at the top show the T waves for the single normal action potential in an example lead V2; each grid square is 0.5 mV tall and 200 ms wide, as in standard ECG paper recordings.